

Calculations of Surface Thermal Expansion*

V. E. Kenner and R. E. Allen

Department of Physics, Texas A&M University, College Station, Texas 77843

(Received 29 December 1972)

Using a method previously described, we have calculated the coefficients of thermal expansion for the first two interplanar spacings near the (111) and (100) surfaces of Ar, Kr, and Xe. The bulk thermal expansion, which is obtained as a by-product in the calculation, is found to be in good agreement with experimental measurements at all temperatures up to the melting point (largely because of a cancellation of errors at higher temperatures). This fact provides some confidence in the method and in the results for the surface thermal expansion. At high temperatures, the results for the surface thermal expansion are in agreement with the prediction of an approximate model which we gave earlier, $\alpha_{\text{surface}}/\alpha_{\text{bulk}} \approx (3/4) \langle u_z^2 \rangle_{\text{surface}} / \langle u_z^2 \rangle_{\text{bulk}}$. At low temperatures, $\alpha_{\text{surface}}/\alpha_{\text{bulk}}$ passes through a rather high peak [with a value of greater than 6 for the (100) surface] because of dispersion of the surface modes. We are not able to give a conclusive explanation of the large apparent discrepancy between our calculations and the experimental observations of Ignatiev and Rhodin, which if taken at face value indicate that $\alpha_{\text{surface}}/\alpha_{\text{bulk}}$ is greater than twice our result of about 1.9 for the (111) surface of Xe between 55 and 75 °K. However, it is possible that factors other than thermal expansion influence the shifts in the Bragg peaks which are observed experimentally, as has been found to be the case in other attempts to measure surface thermal expansion. A nonkinematical calculation of temperature effects in low-energy-electron diffraction from Xe(111) would be of interest in this regard, and also in regard to apparent discrepancies between theoretical and experimental "effective Debye temperatures" at the lowest energies. Experimental observation of the strong peak in $\alpha_{\text{surface}}/\alpha_{\text{bulk}}$ would also be of interest; this peak occurs at roughly 6% of the bulk Debye temperature and should therefore be observable in metals or other materials at cryogenic temperatures.

I. INTRODUCTION

The subject of thermal expansion at a surface has recently received a modest amount of attention.¹⁻⁹ The first theoretical treatments involved minimizing the Helmholtz free energy¹ and carrying out a classical computer experiment.² Both of these methods yielded only the thermal displacements at a single temperature, rather than the thermal-expansion coefficients as functions of temperature. The main finding of these studies was that the rate of thermal expansion must be considerably larger at a surface than in the bulk (for displacements normal to the surface), since the thermal displacements were much larger at the surface for the temperatures and surface orientations studied.

Experimental attempts to measure the rate of thermal expansion near a surface have been reported by Gelatt, Lagally, and Webb³ for Ag(111) and Ni(111), by Woodruff and Seah⁴ for Cu(111), by Wilson and Bastow⁵ for Mo(100) and Cr(100), and by Ignatiev and Rhodin⁶ for Xe(111). These attempts were based on observation of the shifts in the "Bragg peaks" with temperature. Although the results provide evidence that the rate of thermal expansion at the surface exceeds that in the bulk,^{3,5,6} there are other factors besides thermal expansion which influence the shifts in peak positions,^{3,4} so one must be cautious in drawing conclusions from the experimental data.

In the present paper, we apply the method of Ref. 7 in detailed calculations for the (111) and (100) surfaces of the noble-gas solids Ar, Kr, and Xe. We find that our results for the bulk-thermal-expansion coefficients (which are obtained as a by-product) are in good agreement with the experimental values. This fact provides some confidence in the validity of the present method for performing quantitatively accurate calculations.

Recently Dobrzynski and Maradudin⁹ have calculated surface-thermal-expansion coefficients for the (100) surface of α -iron. Since it is difficult to model the ion-ion interactions in iron with any accuracy, the results cannot be regarded as quantitative. In fact, the bulk-thermal-expansion coefficient is found to be in error by a factor of 3. The values for ratios like $\alpha_{\text{surface}}/\alpha_{\text{bulk}}$ should not be so greatly in error, of course. The results of Ref. 9 at high temperatures are, indeed, in good agreement with the prediction

$$\alpha_{\text{surface}}/\alpha_{\text{bulk}} \approx \frac{3}{4} \langle u_z^2 \rangle_{\text{surface}} / \langle u_z^2 \rangle_{\text{bulk}}$$

obtained in Ref. 7.

II. THEORY

The present method, which represents a modification of the one we proposed earlier,⁷ is based on the quasiharmonic approximation, in which the vibrational Helmholtz free energy is given by

$$F_{\text{vib}} = k_B T \sum_{\omega} \ln \left[2 \sinh \left(\frac{\hbar \omega}{2k_B T} \right) \right], \quad (2.1)$$

where k_B is the Boltzmann constant, T is the temperature, and the summation is over the normal-mode frequencies ω of the solid. We assume that the stresses are small enough to be neglected, so that the Gibbs free energy is equal to the Helmholtz free energy F . If Φ is the static energy of the solid, then

$$F = \Phi + F_{\text{vib}}. \quad (2.2)$$

We define a_0 to be an interplanar spacing (i. e., spacing between two planes parallel to the surface) in the bulk and A_i to be the i th interplanar spacing near the surface (with $i=1$ at the surface), and we let

$$A_i = a_0 + a_i, \quad i = 1, 2, \dots \quad (2.3)$$

$$A_0 = a_0. \quad (2.4)$$

(We take the intraplanar spacings to vary in proportion to a_0 , of course.) Then the condition for thermal equilibrium is

$$\frac{\partial F}{\partial a_i} = 0, \quad i = 0, 1, 2, \dots \quad (2.5)$$

We now use a Taylor series expansion of F_{vib} about $a_i = a_i^{(0)}$ and Φ about $a_i = a_i^{(1)}$. (In Ref. 7, we expanded both about $a_i = a_i^{(0)}$.) We assume that the $a_i^{(0)}$ and $a_i^{(1)}$ are chosen in such a way that we can neglect all terms beyond the second. We define

$$\Delta a_i = a_i - a_i^{(0)}, \quad \delta a_i = a_i^{(1)} - a_i^{(0)}. \quad (2.6)$$

Then

$$\frac{\partial \Phi}{\partial a_i} \approx \Phi_i + \sum_j \Phi_{ij} (\Delta a_j - \delta a_j), \quad (2.7)$$

where

$$\Phi_i = \left(\frac{\partial \Phi}{\partial a_i} \right)_1, \quad \Phi_{ij} = \left(\frac{\partial^2 \Phi}{\partial a_i \partial a_j} \right)_1. \quad (2.8)$$

We use the subscript 1 to represent quantities evaluated at $a_i = a_i^{(1)}$ and the subscript or superscript 0 to represent quantities evaluated at $a_i = a_i^{(0)}$. We also have

$$\frac{\partial F_{\text{vib}}}{\partial a_i} \approx \left(\frac{\partial F_{\text{vib}}}{\partial a_i} \right)_0 + \sum_j \left(\frac{\partial^2 F_{\text{vib}}}{\partial a_i \partial a_j} \right)_0 \Delta a_j. \quad (2.9)$$

From (2.2), (2.5), (2.7), and (2.9), we get

$$\sum_j \left[\Phi_{ij} + \left(\frac{\partial^2 F_{\text{vib}}}{\partial a_i \partial a_j} \right)_0 \right] \Delta a_j = - \left[\Phi_i - \sum_j \Phi_{ij} \delta a_j + \left(\frac{\partial F_{\text{vib}}}{\partial a_i} \right)_0 \right]. \quad (2.10)$$

If we represent the terms in square brackets on the left- and right-hand sides of (2.10) by K_{ij} and F_i ,

respectively, (2.10) implies that

$$\Delta a_i = - \sum_j (\bar{K}^{-1})_{ij} F_j, \quad (2.11)$$

where \bar{K} is a matrix having the elements K_{ij} . If we use (2.1) to obtain the derivatives of F_{vib} , we get

$$F_i = \Phi_i - \sum_j \Phi_{ij} \delta a_j - \frac{\hbar}{2A_i^{(0)}} \sum_{\omega_0} \omega_0 \gamma_i(\omega_0) \coth \left(\frac{\hbar \omega_0}{2k_B T} \right), \quad (2.12)$$

$$K_{ij} = \Phi_{ij} + \frac{\hbar}{2A_i^{(0)} A_j^{(0)}} \sum_{\omega_0} \omega_0 \gamma_i(\omega_0) \gamma_j(\omega_0) \times \left[\coth \left(\frac{\hbar \omega_0}{2k_B T} \right) - \left(\frac{\hbar \omega_0}{2k_B T} \right) \text{csch}^2 \left(\frac{\hbar \omega_0}{2k_B T} \right) \right], \quad (2.13)$$

where

$$\gamma_i(\omega) = -A_i \frac{\partial \ln \omega}{\partial a_i}. \quad (2.14)$$

We have assumed in (2.13) that $\partial^2 \ln \omega / \partial a_i \partial a_j \approx 0$. From inspecting typical results for $\partial^2 \ln \omega / \partial a_i \partial a_j$ in our calculations, we estimate that this assumption will ordinarily lead to errors of a few percent.

Once the Δa_i have been determined according to (2.11), the thermal-expansion coefficients

$$\alpha_i = \frac{1}{A_i} \frac{\partial A_i}{\partial T}, \quad i = 0, 1, 2, \dots \quad (2.15)$$

and excess thermal expansion coefficients

$$\Delta \alpha_i = \frac{1}{A_i} \frac{\partial \alpha_i}{\partial T}, \quad i = 1, 2, \dots \quad (2.16)$$

can be determined. We adopt the notation

$$\alpha_{\text{surface}} = \alpha_1, \quad \alpha_{\text{bulk}} = \alpha_0. \quad (2.17)$$

At high temperatures, the second (quantum) term in (2.13) vanishes. At low temperatures, this term will be small compared to the first term (unless the atoms are so light that the zero-point vibrational energy is important compared to the static energy). We therefore have

$$K_{ij} \approx \Phi_{ij}, \quad T \rightarrow 0 \text{ or } T \rightarrow \infty. \quad (2.18)$$

Then (2.11), (2.12), (2.15), (2.16), and (2.18) yield

$$\left. \begin{array}{l} i > 0, \Delta \alpha_i \\ i = 0, \alpha_0 \end{array} \right\} \approx k_B \sum_j (A_i^{(0)})^{-1} (\bar{\Phi}^{-1})_{ij} (A_j^{(0)})^{-1} \times \sum_{\omega_0} \gamma_j(\omega_0) \left(\frac{\hbar \omega_0}{2k_B T} \right)^2 \text{csch}^2 \left(\frac{\hbar \omega_0}{2k_B T} \right), \quad T \rightarrow 0 \text{ or } T \rightarrow \infty. \quad (2.19)$$

In the high-temperature limit (ordinarily valid for $T \gtrsim \Theta_D$, where Θ_D is the bulk Debye temperature), we have

$$\left. \begin{aligned} i > 0, \Delta\alpha_i \\ i = 0, \alpha_0 \end{aligned} \right\} \approx k_B \sum_j (A_i^{(0)})^{-1} (\bar{\Phi}^{-1})_{ij} (A_j^{(0)})^{-1} \sum_{\omega_0} \gamma_j(\omega_0), \quad T \rightarrow \infty. \quad (2.20)$$

We mention that in the context of a crude model, (2.20) implies⁷

$$\frac{\alpha_{\text{surface}}}{\alpha_{\text{bulk}}} \approx \frac{3}{4} \frac{\langle u_z^2 \rangle_{\text{surface}}}{\langle u_z^2 \rangle_{\text{bulk}}}, \quad T \geq \Theta_D \quad (2.21)$$

where $\langle u_z^2 \rangle$ is the mean-square amplitude of vibration normal to the surface.

We now consider low temperatures. One can show that⁷

$$\alpha_i \approx C_i T^3 \int_0^\infty x^4 \text{csch}^2 x dx \propto T^3, \quad T \rightarrow 0 \quad (2.22)$$

where C_i is a constant and

$$x = \hbar\omega/2k_B T. \quad (2.23)$$

[This result follows from the fact that the density of states at low ω is proportional to ω^2 for bulk modes and ω for surface modes, but $\gamma_j(\omega)$ approaches a constant for the bulk modes and is proportional to ω for the surface modes, so the product goes like ω^2 in either case.] Therefore,

$$\alpha_{\text{surface}}/\alpha_{\text{bulk}} \rightarrow \text{constant as } T \rightarrow 0. \quad (2.24)$$

Let ω_{max}^b be the maximum frequency for the bulk acoustic modes. For values of ω near ω_{max}^b , there is dispersion—i. e., if \vec{k} is the wave vector, then ω is smaller than is predicted by the relation $\omega \propto |\vec{k}|$ used in obtaining (2.22). Since $x^2 \text{csch}^2 x$ in Eq. (2.19) increases monotonically as x decreases, it follows that α_{bulk} will be larger than is predicted by (2.22)—i. e., α_{bulk} will increase faster than T^3 at low temperatures. As T continues to increase, however, the contribution of each mode in (2.19) approaches a constant ($x^2 \text{csch}^2 x \rightarrow 1$ as $x \rightarrow 0$), so α_{bulk} will eventually increase much less fast than T^3 . Thus α_{bulk}/T^3 reaches a peak at some temperature T_{peak}^b . The integrand in (2.22) reaches its maximum at $x \approx 2$, or $T \approx \frac{1}{4} \hbar\omega/k_B$, so we expect the maximum deviation from T^3 behavior to occur at some temperature below $\frac{1}{4} \hbar\omega_{\text{max}}^b/k_B$; i. e., we expect $T_{\text{peak}}^b < \frac{1}{4} \hbar\omega_{\text{max}}^b/k_B$. (These same considerations apply to the specific heat at constant volume.¹⁰)

Similarly, let ω_{max}^s be the maximum frequency for the low-lying surface-mode branches. Since the surface modes make a large contribution to α_{surface} , there should be a peak in $\alpha_{\text{surface}}/T^3$ at some temperature T_{peak}^s , and we expect that $T_{\text{peak}}^s < \frac{1}{4} \hbar\omega_{\text{max}}^s/k_B$. Furthermore, we also expect that this peak will be higher than the peak in α_{bulk}/T^3 for the following reasons: (i) There is usually one principal low-lying surface-mode branch, associated largely with vibrations in the direction normal

to the surface, which is of dominant importance. On the other hand, there are three bulk-acoustic-mode branches (roughly speaking, two transverse and one longitudinal). There is, as a result, a relatively narrow range between the frequency at which dispersion begins to become important and the maximum frequency ω_{max}^s in the case of surface modes and a much broader range in the case of the bulk modes. The onset of non- T^3 behavior thus occurs more suddenly in the case of α_{surface} , and we therefore expect the peak in $\alpha_{\text{surface}}/T^3$ to be higher than the peak in α_{bulk}/T^3 . (ii) More important, the surface modes exhibit greater dispersion than the bulk modes, partly because of the static relaxation at the surface which substantially softens the frequencies of the short wavelength surface modes.

In summary, we expect a peak in α_{bulk}/T^3 at a temperature which is low (compared to the Debye temperature $\Theta_D \approx \hbar\omega_{\text{max}}^b/k_B$), a stronger peak in $\alpha_{\text{surface}}/T^3$ at a still lower temperature, and, as a result, a peak in $\alpha_{\text{surface}}/\alpha_{\text{bulk}}$.

III. METHOD OF CALCULATION AND RESULTS

In performing the present calculations for the noble gas solids, we have assumed, as usual, a Lennard-Jones 12-6 potential,

$$\phi(r) = 4\epsilon[(\sigma/r)^{12} - (\sigma/r)^6], \quad (3.1)$$

have performed our calculations for an 11-layer slab with two surfaces, and have determined the frequencies ω in a manner described previously.¹ We could have determined the derivatives $(\partial\omega/\partial a_i)_0$ using first-order perturbation theory, but found it easier just to calculate the frequencies at two values of a_i close to, and on either side of, $a_i^{(0)}$. We used a sample mesh of two-dimensional wave vectors¹ \vec{q} which contains eight and 12 values of \vec{q} in the irreducible element of the two-dimensional Brillouin zone for the (111) and (100) surfaces, respectively. There are thus $3 \times 11 \times 8 = 264$ independent sample frequencies for the (111) surface, and $3 \times 11 \times 12 = 396$ for the (100) surface, which are used in approximating the summation over ω . (This summation contains an infinite number of values of ω for a slab which is infinite in the directions parallel to the surface). Finally, we assumed that the third and deeper interplanar spacings expand in proportion to the bulk interplanar spacing—i. e., we took $\Delta a_i = 0$ for $i \geq 3$ —which is a good approximation.

In test calculations we found that the variation of the static energy (and its derivatives) with the interplanar spacings is more important than the variation of the frequencies (and their derivatives). In our final calculations, we therefore used only one set of $a_i^{(0)}$ —namely, the values corresponding to the positions of static equilibrium—but several values

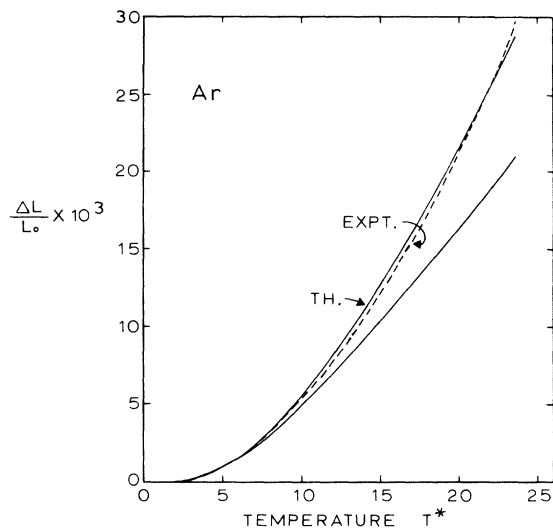


FIG. 1. Bulk thermal expansion of Ar. ΔL is the change in the bulk interplanar spacing from the value L_0 at 0°K ; $T^* = k_B(M\sigma^2/\epsilon)^{1/2} T/\hbar$. The dashed line represents the experimental values of Ref. 12. The lower solid line (unlabeled) represents the "first estimate" described in the text, and the upper solid line (labeled Th.) represents the final calculated results. The Debye temperature for Ar corresponds to $T^* = 26.3$ (see Ref. 17) and the melting point to $T^* = 23.7$ for our choice of ϵ and σ , which is the same as that of Ref. 17.

of δa_i , determined in the way described below to make the Taylor series expansion for $\partial\Phi/\partial a_i$ in (2.7) reasonably accurate at all temperatures. In other words, we expanded $\partial F_{v1b}/\partial a_i$ in (2.9) about

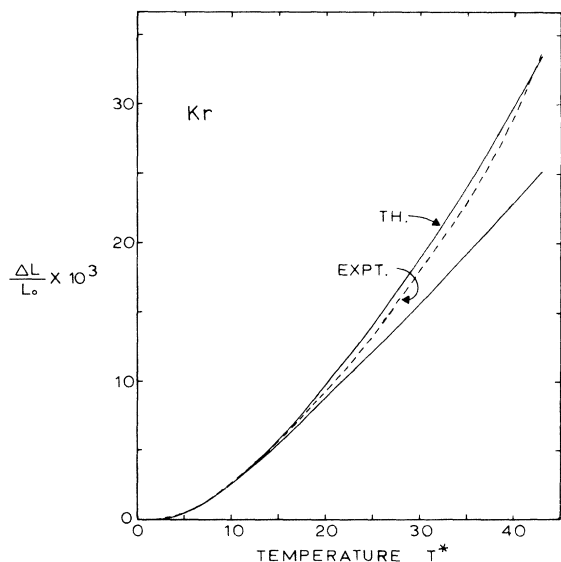


FIG. 2. Bulk thermal expansion of Kr. The notation and labeling are the same as in Fig. 1. The experimental results are from Ref. 13. The Debye temperature corresponds to $T^* = 26.7$ and the melting point to $T^* = 43.3$.

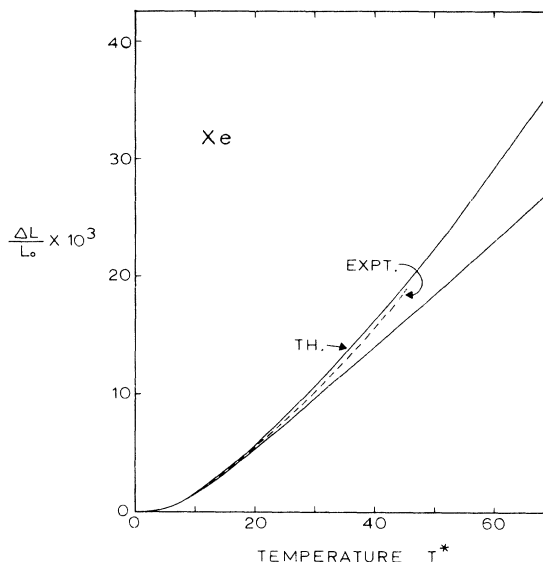


FIG. 3. Bulk thermal expansion of Xe. The notation and labeling are the same as in Fig. 1. The experimental results are from Ref. 11. The Debye temperature corresponds to $T^* = 27.4$ and the melting point to $T^* = 68.9$.

the positions of static equilibrium for all temperatures, but we expanded $\partial\Phi/\partial a_i$ in (2.7) about a number of configurations corresponding to different temperature ranges. All our calculations were based on the full expression Eq. (2.13) for K_{ij} , rather than (2.18).

For the Lennard-Jones potential of Eq. (3.1), we define a dimensionless temperature T^* and a dimensionless thermal-expansion coefficient α^* by

$$T^* = \frac{k_B}{\hbar} \left(\frac{M\sigma^2}{\epsilon} \right)^{1/2} T, \quad (3.2)$$

$$\alpha_i^* = \frac{1}{A_i} \frac{dA_i}{dT^*}, \quad (3.3)$$

where M is the atomic mass.

Our procedure consisted of two steps: To obtain a first estimate of the interplanar spacings, we expanded both $\partial F_{v1b}/\partial a_i$ and $\partial\Phi/\partial a_i$ about the static equilibrium configuration. This first estimate gave the results for the bulk indicated by the unlabeled solid lines in Figs. 1-3 and by the solid lines in Figs. 4-6. Notice that the curve for α_{bulk}^* unphysically levels off to a constant value at high temperatures. (We do not show the results for the first estimate of α_1^* and α_2^* .) Then, using the values of the interplanar spacings obtained in this estimate (Figs. 1-3) at several values of the temperature (e.g., $T^* = 20, \dots, 70$ for Xe), we took the δa_i of (2.6) and (2.7) to have the corresponding values in our final calculation of the Δa_i at these temperatures; i.e., in finally determining the thermal-expansion coefficient.

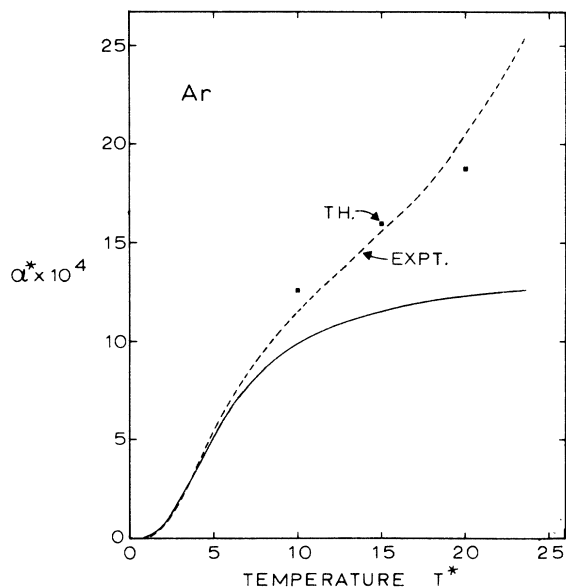


FIG. 4. Bulk-thermal-expansion coefficient of Ar vs temperature. Here $\alpha_{\text{bulk}}^* = A_0^{-4} (dA_0/dT^*)$. The dashed line represents the experimental results of Ref. 12. The lower solid line represents the "first estimate" described in the text. The squares represent the final calculated values, determined in the way described in the text.

coefficients α_i^* at a given temperature, we expanded $\partial\Phi/\partial a_i$ about the configuration which was predicted in our first estimate for this temperature. However,

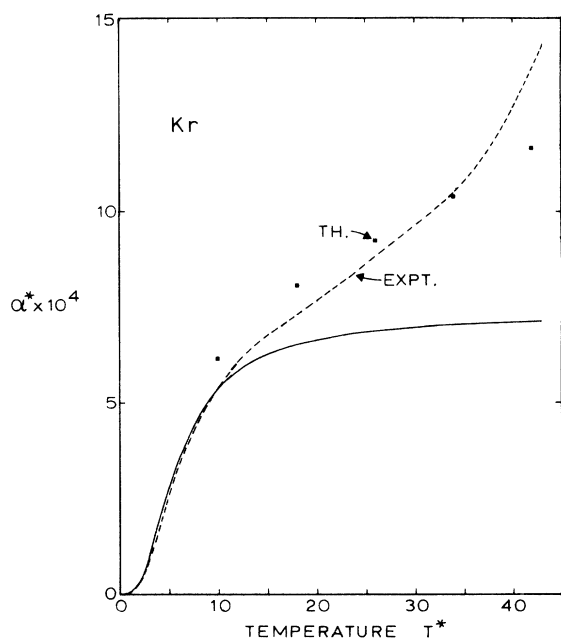


FIG. 5. Bulk-thermal-expansion coefficient of Kr vs temperature. The notation and labeling are the same as in Fig. 4. The experimental results are from Ref. 13.

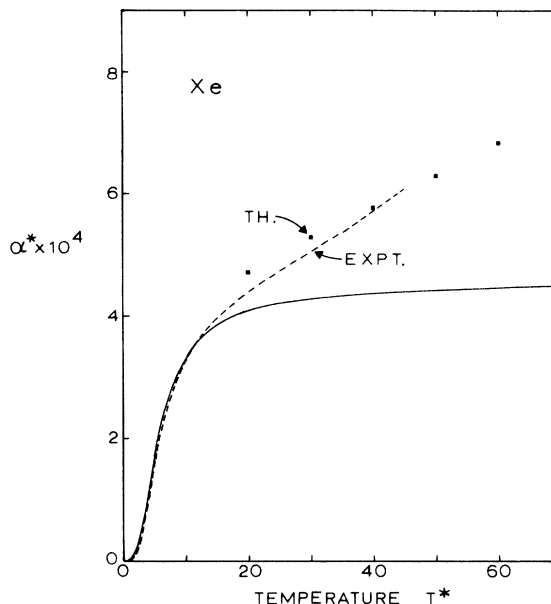


FIG. 6. Bulk-thermal-expansion coefficient of Xe vs temperature. The notation and labeling are the same as in Fig. 4. The experimental results are from Ref. 11.

as mentioned above, we always expanded $\partial F_{\text{vib}}/\partial a_i$ about the configuration of static equilibrium.

In the case of α_{bulk}^* , the results from the above procedure are indicated by the squares in Figs. 4-6 (e.g., at $T^* = 20, 30, \dots, 60$ for Xe). The experimental results¹¹⁻¹³ are indicated by the dashed lines. For temperatures somewhat below melting, our results are in remarkably good agreement with experiment. Even near the melting temperature our results are too low by a maximum of about 18% for Ar and 14% for Kr. (We find no reliable experimental data for Xe near melting.) This agreement with the bulk experimental data provides some confidence in our approximations and in our results for the surface thermal-expansion coefficients.

In order to obtain values of the expansion coefficients α_i between those determined at a small number of sample temperatures ($T^* = 20, \dots, 70$ for Xe) in the way described above, we have simply interpolated between the sample temperatures using a cubic interpolation formula.¹⁴ The results obtained in this way were then integrated to obtain the fractional interplanar expansions $\Delta L/L_0$ (the labeled theoretical curves in Figs. 1-3 and 7-9). The bulk values of $\Delta L/L_0$ agree much better with experiment than do the results for the expansion coefficients, of course, since the integrated quantity does not change as rapidly as the integrand.

We mention that our results for α_{bulk}^* at high T are considerably better than those obtained from much more elaborate calculations based on the quasi-harmonic approximation,¹⁵ because of a cancella-

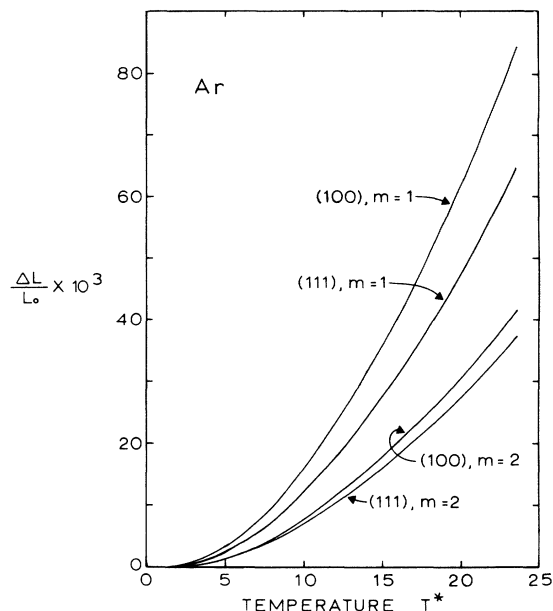


FIG. 7. Surface thermal expansion for the first ($m=1$) and second ($m=2$) interplanar spacings. These results are for the (100) and (111) surfaces of Ar. ΔL is the change in the first or second interplanar spacing from the value L_0 at 0°K .

tion of errors in our method: As can be seen in Figs. 1–3, our first estimate of the interplanar spacing is well below the correct value at high T . As a result, our final calculated values of α_{bulk} will be too small. On the other hand, the quasiharmonic approximation (plus the Lennard-Jones potential) predicts values of α_{bulk} which are too large.¹⁵ The monic approximation (plus the Lennard-Jones poten-

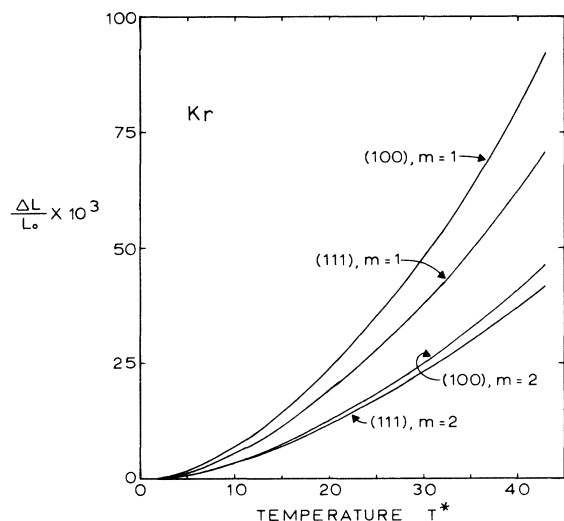


FIG. 8. Surface thermal expansion for Kr.

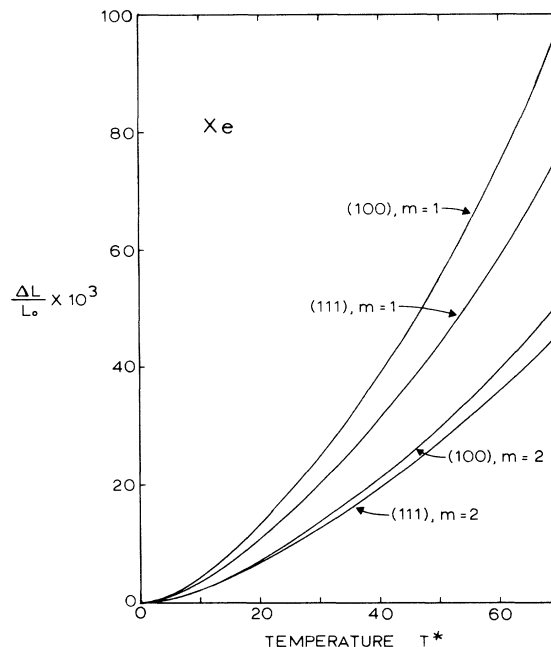


FIG. 9. Surface thermal expansion for Xe.

tial) thus tend to cancel, so that our results are more accurate than those obtained in more rigorous calculations based on the quasiharmonic approximation.

The bulk results shown in Figs. 1–6 were obtained for a slab having a (111) surface orientation, but the results obtained for a slab with a (100) orientation are almost identical to these, as must be the case if our method is to be reliable. One might expect our results for the surface expansion coefficients to have the same general agreement with experiment as our bulk results (i. e., very good agreement at low temperatures and moderately good agreement at higher temperatures), although we do expect the quasiharmonic approximation to fail at lower temperatures at the surface because the amplitudes of vibration are larger.

In obtaining results for the surface thermal expansion we assumed the "first estimate" to fail at the same temperature for the surface as it did for the bulk (i. e., $T^* = 5, 10, \text{ and } 10$ for Ar, Kr, and Xe, respectively). The results obtained for the first two interplanar spacings and for the (111) and (100) surfaces are shown in Figs. 7–9 for temperatures up to the melting temperature ($T = 84, 116, \text{ and } 161^\circ\text{K}$ for Ar, Kr, and Xe, respectively). For all three materials and both interplanar spacings, the expansion is greater for the (100) surface than the (111); this difference we attribute to the fact that there are more surface modes with lower frequencies for the (100) surface¹⁶ and, more important, that the surface modes exhibit greater dispersion for the (100) surface.

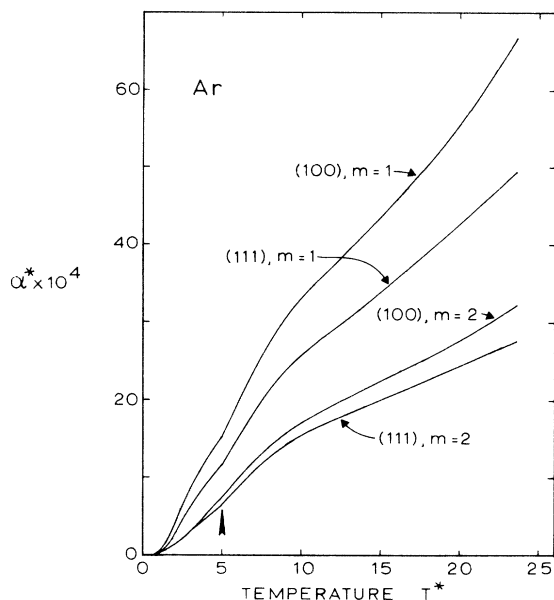


FIG. 10. Thermal-expansion coefficients for the first ($m=1$) and second ($m=2$) interplanar spacings beneath the surface. These results are for the (111) and (100) surfaces of Ar. To the left of the vertical arrow, the results were obtained by expanding $\partial\Phi/\partial a_i$ about the positions of static equilibrium, and to the right by the interpolation scheme described in the text.

The results for the surface expansion coefficients are shown in Figs. 10–12, with the arrow indicating the temperature below which the “first estimate” described above was used. Above this temperature the surface expansion coefficients were calculated at a few sample temperatures, as ex-

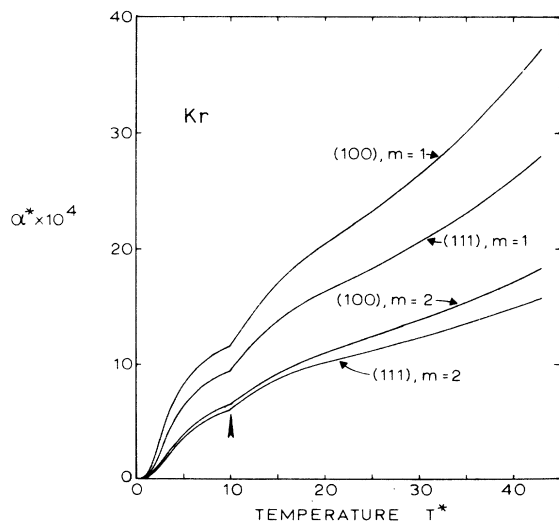


FIG. 11. Surface-thermal-expansion coefficients for Kr. The notation and labeling are the same as in Fig. 10.

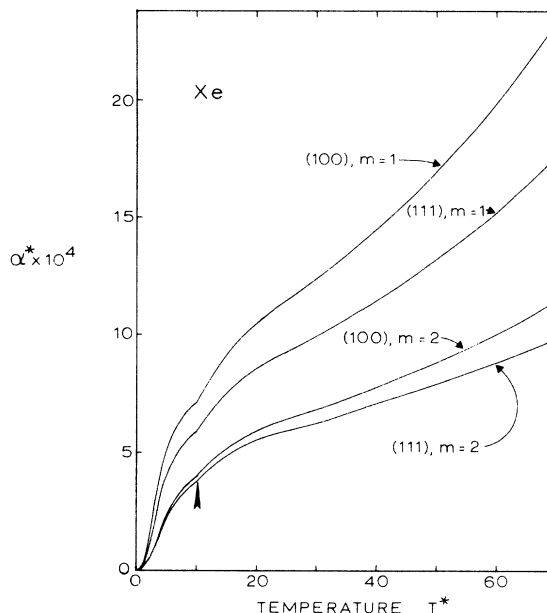


FIG. 12. Surface-thermal-expansion coefficients for Xe. The notation and labeling are the same as in Fig. 10.

plained above, and a cubic interpolation gave the values plotted at intermediate temperatures.¹⁴

In Fig. 13, the ratios $\alpha_{\text{surface}}/\alpha_{\text{bulk}}$ and $\alpha_2/\alpha_{\text{bulk}}$ are plotted for the (111) and (100) surfaces of Xe. Similar results for Ar and Kr are not plotted, since the curves for these materials are nearly the same as those for Xe. (The ratios for Ar and Kr differ from those for Xe by a maximum of 6% when plotted versus T^* .) Two points regarding Fig. 13 are worth noting: First, the ratio $\alpha_{\text{surface}}/\alpha_{\text{bulk}}$ increases with temperature at high temperatures. Comparison with calculated values¹⁷ of the mean-square amplitudes of vibration in the direction normal to the surface, $\langle u_z^2 \rangle_{\text{surface}}$ and $\langle u_z^2 \rangle_{\text{bulk}}$ for atoms, respectively, in the surface layer and in the bulk, show that the results of Fig. 13 are in approximate agreement with (2.21): $\alpha_{\text{surface}}/\alpha_{\text{bulk}} \approx \frac{3}{4} \langle u_z^2 \rangle_{\text{surface}} / \langle u_z^2 \rangle_{\text{bulk}}$. Second, as $T \rightarrow 0$ $\alpha_{\text{surface}}/\alpha_{\text{bulk}}$ undergoes a large increase, passes through a peak at roughly 6% of the bulk Debye temperature,¹⁸ and then decreases again. The reason for this behavior is dispersion of the low-frequency surface modes, as discussed in Sec. II. We mention that $\omega_{\text{max}}^* = (M\sigma^2/\epsilon)^{1/2} \omega_{\text{max}}^s$ is about 10 for both the (111) and (100) surfaces,¹⁶ where ω_{max}^s is the maximum surface-mode frequency for the low-lying branches, so according to the arguments of Sec. II the peak should occur below $T^* = \frac{1}{4} \omega_{\text{max}}^* = 2\frac{1}{2}$, as it does. There are more surface modes for the (100) surface than there are for the (111) surface, the (100) surface modes show greater dispersion, and the surface-mode frequencies are lower (on the average) for the (100)

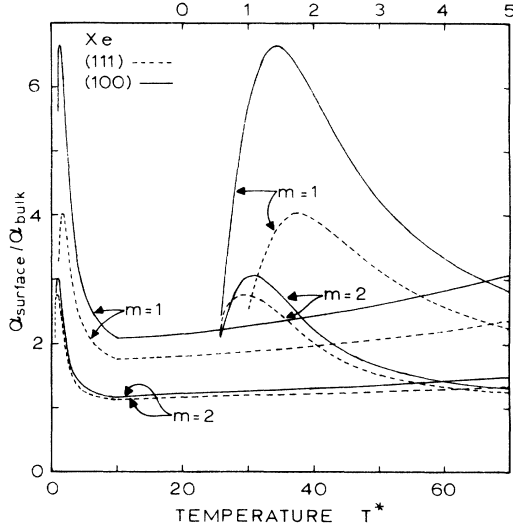


FIG. 13. Ratio of α for first ($m=1$) and second ($m=2$) interplanar spacings to α_{bulk} . These results are for Xe(111) and Xe(100). On the right-hand side, we use the expanded scale at the top to show the behavior at low temperatures ($0 < T^* \leq 5$). The slight discontinuity at $T^*=10$ (in the graphs for $0 < T^* \leq 70$) is due to a change in method at this point, as discussed in the text and in the caption to Fig. 10.

surface.¹⁶ The arguments of Sec. II indicate that, as a result, the peak should be higher and should occur at a slightly lower temperature for the (100) surface, as is the case. Below the peak, $\alpha_{\text{surface}}/\alpha_{\text{bulk}}$ should approach a constant as $T \rightarrow 0$, according to (2.24). However, our results at very low temperatures are unreliable because we used a slab of finite thickness and a finite mesh of sample points in performing the calculations, so we cannot check this conclusion.

In Fig. 14, we plot $\alpha_{\text{bulk}}^*/T^{*3}$, $\alpha_{\text{surface}}^*/T^{*3}$, and α_2^*/T^{*3} for the (111) and (100) surfaces of Xe. There is only a small deviation from T^3 behavior for α_{bulk} and a much greater deviation for α_{surface} and α_2 at low T . Also, there is a much larger deviation from T^3 behavior for the (100) surface than for the (111) surface; this result we again attribute to the greater dispersion of the surface modes for the (100) orientation, so that their effect is more pronounced. The fact that α_2/T^3 peaks at a lower temperature than $\alpha_{\text{surface}}/T^3$ can be attributed to the fact that the attenuation of the surface modes increases with ω . At first the surface modes will contribute more and more heavily to α_2 as ω increases and their penetration decreases. However, when ω increases beyond a certain point, the surface modes are so localized near the surface that they make little contribution to α_2 . Consequently, as ω (or T) increases, the surface modes will make their heaviest contribution to α_2 before they make

their heaviest contribution to α_{surface} , and so α_2 peaks at lower T .

IV. CONCLUSION

The three main qualitative conclusions of the present paper are the following: (i) Our method yields results which are in good agreement with the measured values of the bulk thermal-expansion coefficients for Ar, Kr, and Xe. (ii) At high temperatures, the results are in approximate agreement with the prediction $\alpha_{\text{surface}}/\alpha_{\text{bulk}} \approx \frac{3}{4} \langle u_g^2 \rangle_{\text{surface}} / \langle u_g^2 \rangle_{\text{bulk}}$. (iii) At low temperatures, there is a strong peak in $\alpha_{\text{surface}}/T^3$ and in $\alpha_{\text{surface}}/\alpha_{\text{bulk}}$.

Recently, Ignatiev and Rhodin^{6(a)} inferred the rate of surface thermal expansion for Xe(111) by observing the shifts in the low-energy-electron-diffraction (LEED) "Bragg peaks" with temperature. Their result was $\alpha_{\text{surface}}/\alpha_{\text{bulk}} \approx 4$ or 5 (or even larger) between 55° and 75° K, which is much larger than our result of about 1.9 in the same range (see Fig. 13). Although we cannot rule out the possibility that this apparent discrepancy is caused by some failing in our calculations, we feel that it is more likely due to difficulties in interpreting the experimental data, for the following reasons.

The three principal approximations in our method are (i) the quasiharmonic approximation, (ii) the

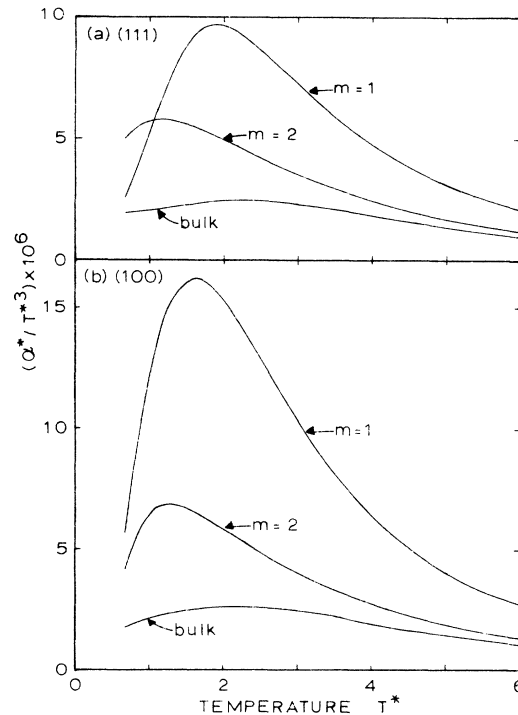


FIG. 14. Ratios $\alpha_{\text{bulk}}^*/T^{*3}$, $\alpha_{\text{surface}}^*/T^{*3}$ ($\alpha_{\text{surface}} = \alpha_1$), and α_2^*/T^{*3} for the (111) and (100) surfaces of Xe. T^* and α^* are the dimensionless quantities defined in the text (and in the captions to Figs. 1 and 4).

use of a truncated Taylor series expansion about our "first estimate" of the atomic positions, and (iii) the assumption of a two-body Lennard-Jones interaction. Both of the first two approximations should break down at lower temperatures at the surface than in the bulk, since the vibrational amplitudes and change in the interplanar spacings (from the values at 0 °K) are larger at the surface. However, we expect that there will be appreciable cancellation of the error in the quasiharmonic approximation (plus the Lennard-Jones potential) and the error in the use of a truncated Taylor series, as there is for the bulk thermal expansion. If so, the total error in α_{surface} at one-third the melting point (i.e., 50 or 60 °K) should not exceed by very much the error in α_{bulk} at the melting point, which is about 15%.

It is difficult to believe that the Lennard-Jones potential is much less accurate at the surface than in the bulk, since this would imply that the effective two-body interaction at the surface and in the bulk are greatly different. In a metal, it is not unreasonable that the effective ion-ion interaction may be different in the surface layer from what it is in the bulk, since the valence electrons screen this interaction and the states of the valence electrons will be strongly affected by the surface. However, in a molecular solid such as Xe, the electronic states are less affected by the environment, and one expects the effective atom-atom interaction to be approximately the same at the surface and in the bulk. Of course, there are contributions from three-body forces, etc. in the effective two-body interaction, and these contributions will be changed by the environment. However, we do not expect the change to be enough to have a drastic effect on the net effective interaction between atoms.

We conjecture that the apparent discrepancy between our results for $\alpha_{\text{surface}}/\alpha_{\text{bulk}}$ and the value inferred by Ignatiev and Rhodin is due principally to multiple scattering and other effects which invalidate a simple kinematical analysis of the data. In many ways the scattering from Xe(111) is nearly kinematical, and certainly more nearly kinematical than the scattering from most materials.⁶ However, it is clear that there are nonkinematical features in the data.⁶ In particular, there is strong evidence of nonkinematical behavior around the (333) peak [see Fig. 4 of Ref. 6(a)]. If the (444) and (555) peaks also were nonkinematical, in so far as shifts in the Bragg peaks are concerned, then it would not

be valid to infer a high rate of surface thermal expansion from the data in Figs. 12 and 14 of Ref. 6(a).

We mention another interesting fact which may indicate that the (444) and (555) peaks show nonkinematical behavior—in this case, with regard to changes in the peak height (rather than peak position) with temperature¹⁹: In Fig. 7 of Ref. 6(b), the measured $\Theta_{D,\text{eff}}$ (effective Debye temperature) is plotted as a function of electron energy and is compared with calculated values which were obtained from the theoretical mean-square amplitudes of Refs. 1 and 2 (after adjustment of the theoretical bulk values). The better theoretical values are presumably those of Ref. 2, since these values include anharmonic effects. The experimental values of $\Theta_{D,\text{eff}}$ and the theoretical values (based on Ref. 2) agree very well for the (666) and higher peaks. However, there are noticeable discrepancies for the (444) and (555) peaks. In model calculations, Laramore and Duke²⁰ obtained nonkinematical contributions to the effective Debye temperature which are of the same order of magnitude as these discrepancies (~5–10%).

We therefore reach the conclusion that the apparent discrepancies between theory and experiment for Xe(111) can be resolved for both the surface thermal expansion and the surface mean-square amplitudes of vibration, if we assume that there are appreciable nonkinematical contributions to the shifts of the peak positions and the peak heights with temperature for the (333), (444), and (555) "Bragg" peaks. A nonkinematical calculation of temperature effects in LEED from Xe(111) would be of great interest.

We also mention that it should be possible to observe the large peaks in $\alpha_{\text{surface}}/T^3$ and $\alpha_{\text{surface}}/\alpha_{\text{bulk}}$ (see Figs. 13 and 14) at cryogenic temperatures in metals or other materials. The peak in $\alpha_{\text{surface}}/\alpha_{\text{bulk}}$ should occur at roughly 6% of the Debye temperature, according to our results. Such a measurement would amount to an indirect observation of low-frequency surface modes and their dispersion.

ACKNOWLEDGMENT

The authors are very much indebted to Professor T. N. Rhodin and Dr. A. Ignatiev for providing us with a copy of Dr. Ignatiev's Ph.D. thesis and with preprints of Ref. 6. We wish to emphasize that the comments in Sec. IV are not intended to detract from this excellent piece of work.

*Work supported in part by a grant from the Texas A&M Research Council.

¹R. E. Allen and F. W. deWette, Phys. Rev. **179**, 873 (1969).

²R. E. Allen, F. W. deWette, and A. Rahman, Phys. Rev. **179**, 887 (1969).

³C. D. Gelatt, M. G. Lagally, and M. B. Webb, Bull. Am.

Phys. Soc. **14**, 793 (1969).

⁴D. P. Woodruff and M. P. Seah, Phys. Status Solidi A **1**, 429 (1970).

⁵J. M. Wilson and T. J. Bastow, Surf. Sci. **26**, 461 (1971).

⁶(a) A. Ignatiev and T. N. Rhodin, Phys. Rev. B **8**, 893 (1973);
(b) S. Y. Tong, T. N. Rhodin, and A. Ignatiev, Phys. Rev. B **8**,

- 906 (1973).
- ⁷R. E. Allen, *J. Vac. Sci. Technol.* **9**, 934 (1972); and unpublished.
- ⁸V. E. Kenner and R. E. Allen, *Phys. Lett. A* **39**, 245 (1972).
- ⁹L. Dobrzynski and A. A. Maradudin, *Phys. Rev. B* **7**, 1207 (1973).
- ¹⁰A. A. Maradudin, E. W. Montroll, G. H. Weiss, and I. P. Ipatova, *Theory of Lattice Dynamics in the Harmonic Approximation*, 2nd ed. (Academic, New York, 1971), pp. 136–137.
- ¹¹C. R. Tilford and C. A. Swenson, *Phys. Rev. B* **5**, 719 (1972).
- ¹²O. G. Peterson, D. N. Batchelder, and R. O. Simmons, *Phys. Rev.* **150**, 703 (1966).
- ¹³D. L. Losee and R. O. Simmons, *Phys. Rev.* **172**, 944 (1968).
- ¹⁴For $T^* < T_0^*$, with $T_0^* = 5, 10,$ and 10 for Ar, Kr, and Xe, respectively, the values of ΔL and α^* obtained in the “first estimate” are given in Figs. 1–3 and 7–12. For $T^* > T_0^*$, the values were obtained by interpolation.
- ¹⁵M. L. Klein, G. K. Horton, and J. L. Feldman, *Phys. Rev.* **184**, 968 (1969).
- ¹⁶R. E. Allen, G. P. Alldredge, and F. W. deWette, *Phys. Rev. B* **4**, 1661 (1971). Compare Figs. 8 and 10. There are two prominent low-frequency surface mode branches for the (100) surface and only one for the (111) surface.
- ¹⁷R. E. Allen and F. W. deWette, *Phys. Rev.* **188**, 1320 (1969), see Table III.
- ¹⁸For Xe, $(k_B / \hbar) (M\sigma^2/\epsilon)^{1/2} \Theta_D = 27.4$, where Θ_D is the bulk Debye temperature. (See Ref. 17). The peak in $\alpha_{\text{surface}}/\alpha_{\text{bulk}}$ is at about 1.43 for the (100) surface and 1.75 for the (111) surface.
- ¹⁹A. Ignatiev, S. Y. Tong, T. N. Rhodin, B. I. Lundqvist, and J. B. Pendry, *Solid State Commun.* **9**, 1851 (1971).
- ²⁰G. E. Laramore and C. B. Duke, *Phys. Rev. B* **2**, 4783 (1970).